A. Airoldi, P. Bettini, P. Panichelli, G. Sala
Chiral Topologies for Composite Morphing Structures - Part II: Novel Configurations and Technological Processes
Physica Status Solidi. B, Basic Solid State Physics, Vol. 252, N. 7, 2015, p. 1446-1454
doi:10.1002/pssb.201584263

CHIRAL TOPOLOGIES FOR COMPOSITE MORPHING STRUCTURES - PART II: NOVEL CONFIGURATIONS AND TECHNOLOGICAL PROCESSES

Alessandro Airoldi*, Paolo Bettini*, Paolo Panichelli*, Giuseppe Sala*
***Dept. of Aerospace Science and Technology, Politecnico di Milano**
Via La Masa, 34 – 20156 Milano - Italy

Abstract

The paper presents the advancements in the technological processes developed to produce chiral honeycombs made of thin composite laminates. An original technological process, which was applied to produce chiral components for aerospace morphing structures, is critically analysed and a new approach is proposed. The objective of such approach is the production of thin-walled chiral composite structures with enhanced strength properties by using a more feasible technology. According to the new methodology, chiral honeycombs with polygonal nodes are obtained by assembling thin-walled prismatic composite tubes. Numerical models are developed to investigate the behaviour of such topologies. A comparison with the performances of chiral honeycombs with cylindrical nodes is presented, showing that the new configuration can provide negative Poisson's ratios that tend to the theoretical limit of -1 as the stiffness of the polygonal nodes is increased. Thereafter a method to fill partially the nodes is proposed and numerically assessed, to enhance at the same time the auxetic behaviour and the mechanical properties of the chiral honeycomb. Finally a complete manufacturing process is developed. Hexa-chiral structural units are manufactured and subsequently tested to assess the auxetic response. Results are in acceptable agreement with numerical predictions and indicate that the novel technological route provides a significant contribution for the application of composite chiral honeycomb to morphing structures.

1 Introduction

Chiral topologies represent a possible solution to develop systems that exhibit negative Poisson's ratios, a behaviour that is physically admissible but is not displayed by conventional materials used in structural engineering. The possibility to obtain a negative Poisson's ratio was demonstrated at the molecular level by Wojciechowski [1], considering hexamers with a chiral structure, which could not be superposed to its mirror image [2]. Such concept was extended to mechanical structures by Lakes [3], who replaced molecules with circular elements, denoted as nodes, and atomic interactions with tangential ligaments that connect the nodes according to a non-centrosymmetric scheme [3,4]. A scheme based on a hexagonal array of ligaments converging at each node can be repeated to form a plane tessellation, which is characterized by a periodic cellular structure and generates a hexa-chiral honeycomb. When such structure is compressed, ligaments tends to wind on the nodes, thus contracting the honeycomb in the transversal direction, whereas a tensile loading induces the unwinding of the ligament and a consequent transversal expansion. At the meta-material level, the resulting negative Poisson's ratio involves an increment of the shear modulus of elasticity, so that an auxetic chiral honeycomb can be expanded or contracted but inherently opposes to local shape variations. A similar response is also obtained by other types of chiral topologies, as summarized in [5] by Alderson et al., and anisotropic tessellations can be applied to achieve values of Poisson's ratio lower than -1 (see Pozniak and Wojciechowski [6]).

From the applicative point of view, the auxetic response that characterizes chiral topologies has appealing characteristics for aerospace morphing structures that can progressively change their shape to interact more efficiently with the airflow. Among the several types of morphing solutions that have been devised by researchers in the last decades [7, 8], the development of wings hosting chiral honeycomb core was proposed by several authors to obtain smooth and

controlled variations of the camber of an airfoil [9-14]. Such property was exploited to optimize the generation of aerodynamic forces in given conditions or to control the aircraft with a seamless transformation of the aerodynamic surfaces. .

Indeed, a barrier to the application of chiral topologies is represented by technological issues, since manufacturing of a honeycomb with a non-centrosymmetric topology cannot be easily obtained. Rapid prototyping techniques have been used to produce and investigate different types of polymeric chiral honeycombs [10,15], but mechanical properties of such materials do not meet the highly demanding material requirements for aerospace applications and are subjected to significant variations with technological parameters [16]. Metallic chiral honeycombs were produced by machining solid plates, as in Spadoni and Ruzzene [11], though the process is time and material consuming and presents several limitations.

The adoption of composite materials increases the potential performances and the design flexibility of chiral honeycombs, as it was shown by Bettini et al. [14], and allows the application of different manufacturing strategies. The Resin Transfer Moulding (RTM) technology described in Cicala et al. [17] is suited to manufacture composite chiral honeycombs with composite materials, although the thickness of the ligaments that can be produced cannot be easily reduced below certain limits, due to the characteristic of RTM process.

The development of the chiral rib presented in the part I of the this work was based on a technology for the production of thin-walled chiral composite honeycomb, which was originally devised in Bettini et al. [14] and also applied in Airoldi et al. [18]. Such process is based on the separate production of curved ligaments that are subsequently superimposed and bonded in a second curing cycle. Although this manufacturing approach was successfully applied to produce a complete chiral rib with a wall thickness of 0.5 mm, it is characterized by a significant complexity and the risk of ligament debonding represent a structural weak point.

Moving from these results, this paper presents further steps towards the application of composite chiral honeycombs. An innovative version of the composite chiral network is proposed. Numerical, technological and experimental activities are presented to show that the proposed innovation simplifies the technological process and is particularly promising to enhance the mechanical properties of composite chiral networks.

In the following section of this paper, the original technological process is critically analysed and a novel approach to obtain a hexa-chiral tessellation is presented. Thereafter, numerical studies are applied to investigate and improve the auxetic response of the hexa-chiral configurations that can be obtained by applying the new technological route. Finally, the manufacturing process is developed to produce chiral units by using two different composite materials, which are subsequently tested. The main findings are summarized in a conclusive section.

2 Chiral configurations with polygonal nodes

The development and the application of the technology for thin-walled composite chiral networks, described in Bettini et al. [14] and Airoldi et al.[18] pointed out some problematical aspects of the manufacturing process and of the produced components. In the companion paper that presents the part I of this work, the process was successfully applied to manufacture a chiral network with more than two hundreds ligaments. However, the process resulted very time-demanding, particularly for the preparation of the final assembly mould, which requires high precision in the positioning of adhesive films and rubber inserts. Additionally, bonding between ligaments represents an inherent critical weak point in the structural concept. It is worth remarking that mechanical tests proved that the application of elastomeric inserts during the bonding process leads to very good adhesion quality, since tensile failures occurred when ligaments were close to their bending ultimate strength. However, the cusps at the tangency points of the chiral network represent a critical location for fracture development, so

that behaviour under cyclic loadings or in more severe environmental conditions could be characterized by unacceptable strength levels for real-world applications.

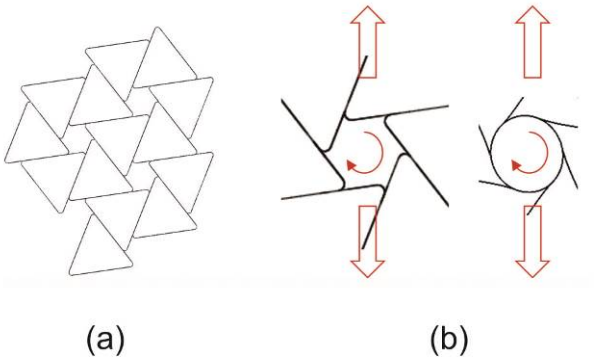

Fig. 1–Chiral configuration with hexagonal nodes (a) and comparison with conventional configuration under tension (b)

Such considerations motivated the development of an alternative method to obtain the hexa-chiral topology by using thin composite laminates. The new approach is based on a tessellation created by adjoining polygonal shapes, as the triangles shown in Fig. 1-a. A proper positioning of such triangles creates a non-centrosymmetric topology with hexagonal nodes connected by ligaments that are parallel to their sides. The result is a hexa-chiral topology where cylindrical nodes are substituted by polygonal one, thus obtaining a geometry similar to the one produced by using the RTM process presented in Cicala et al. [17]. It can also be observed that analogous tessellations could be proposed for other types of chiral topologies, such as in the tetra-chiral or anti-tetra chiral cases [5, 6], which could be obtained by adjoining square or rectangular elements.

A potential advantage of the new technological concept is envisaged considering that the positioning of polygonal shapes and the subsequent bonding along their straight sides could facilitate the assembly process. Additionally, in the new type of topology, cusps should tend to close in tensile load conditions, as it sketched in Fig 1-b. Moreover, cusps are now oriented

towards the interior of the nodes, so that a filler introduced inside the nodes will increase the strength of the cusps without interfering with the compliance of the ligaments.

3 Numerical studies for the novel configuration

The considerations introduced in the previous section motivated a numerical study aimed at evaluating the auxetic behaviour that can be obtained by a composite hexa-chiral network produced by adjoining thin-walled triangular tubes. A conventional hexa-chiral chiral topology characterized by r = 5 mm and L = 25 mm, where r is the diameter of the node and L the ligament length, was selected to be compared with a configuration having polygonal nodes. In the new configuration the radius r is equal to the apothem of the hexagon and the length of the ligament is measured from the mid-point of the side of hexagon. Indeed, the free length of the ligament is lower in the tessellation with hexagonal nodes with respect to the more conventional geometry with cylindrical nodes, so that the new configuration is expected to be stiffer than the conventional one. The SEAL CC90/ET445 carbon fabric material with the properties reported in Table 1 was selected for the comparative study, considering a generic homogeneous lamination sequence $[0]_n$ and a ligament thickness of 0.3 mm.

Table 1 – Properties of the composite plies used for the development of the technology

		Carbon fabric	Glass fabric
E_{11}	MPa	56550	24000
E_{22}	MPa	56550	24000
ν_{21}	-	0.05	0.11
G_{12}	MPa	4040	4043
ply thickness	mm	0.1	0.055

However, in the numerical analyses the thickness of the node walls was varied to increase the stiffness of the nodes, since it is known that the theoretical limit of -1 Poisson's ratio, can be

approached if nodes are considerably stiffer than the ligaments as demonstrated by Prall and Lakes [4].

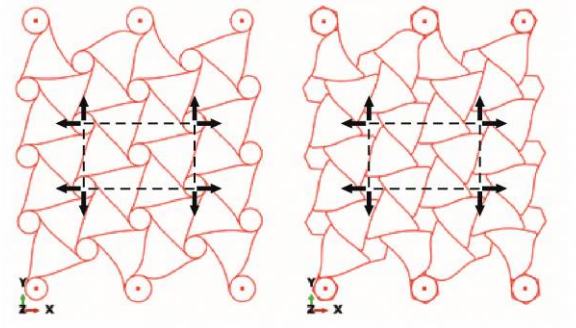

Fig. 2– Models of chiral networks with circular and hexagonal nodes

Considering possible experimental assessments, a chiral network with finite dimensions was taken into account for the numerical studies. The finite element models of the considered chiral networks with circular and hexagonal nodes were developed to be solved by using the Simulia/Abaqus Standard code [19] and are presented in Fig. 2. First-order shell elements were used (*S4* elements [19]) and typical element size was set to about 1.5 mm. The width of the network was set to 10 mm. The nodes of the finite element meshes in the three lower cylinders and in the three upper cylinders of the conventional model were connected to six central reference nodes. Kinematic constraints were set to force the cylinders to rotate as they were rigidly connected to pins with axes passing through the reference nodes, without constraining their radial deformation. The same constraints were applied in the configuration with polygonal nodes. The vertical displacements of the three lower reference nodes were fixed, whereas, at the upper end, an identical given displacement was imposed to all the three reference nodes. The horizontal displacements of all the reference nodes were left free, excluding one node that was constrained to eliminate the rigid body motion of the entire network. According to such system of constraints, the chiral networks are free to contract or expand in the horizontal direction and all the chiral nodes are free to rotate and radially deform.

The Poisson's ratio of the networks was estimated by considering the displacements of the centres of the chiral nodes at the four vertices of the dashed rectangles shown in Fig. 2, which are positioned in the central part of the structure. In all the numerical analyses presented in this section, the total engineering strains at the end of the computations were evaluated from such displacement to calculate the Poisson's ratio. For each chiral node, the positions of the centres were evaluated by averaging the coordinates of two couples of points set in diametrical positions along the perimeter of the node, in the undeformed and deformed configuration.

The results of the study are presented in Table 2, where the stiffness of the network is calculated by dividing the sum of the vertical forces obtained at the three upper vertical nodes by the imposed common displacement.

It can be observed that the auxetic responses of the topologies with circular and hexagonal nodes are very similar, though the conventional configuration is significantly more compliant than the one with hexagonal nodes, as it was expected. The increment of the wall thickness of the hexagonal nodes enhances the auxetic behaviour of the network. Such behaviour can be related to the increment of the material volume fraction in the chiral topology, which is known to be one most important factors affecting the mechanical properties of metamaterials, as it is exemplified in the studies presented in [20, 21 and 22].

Table 2 – Auxetic behaviour of configurations with hexagonal nodes

Types of nodes	Ligament thickness (mm)	Node thickness (mm)	Stiffness (N/mm)	Network Poisson's ratio
Circular	0.3	0.4	32.7	-0.467
Hexagonal	0.3	0.4	77.4	-0.455

Hexagonal	0.3	0.6	87.8	-0.743

The contour of the longitudinal stress components shown in Fig. 3 is referred to the case with hexagonal nodes, a ligament thickness of 0.3 mm and a nodal thickness of 0.4 mm. It can be observed that the sides of the hexagon converging at the cusps of the nodes are bended in the same direction, so that the tendency to open a mode I crack in the adhesive layer is reduced with respect to the conventional configuration with ligaments that are tangent to circular nodes.

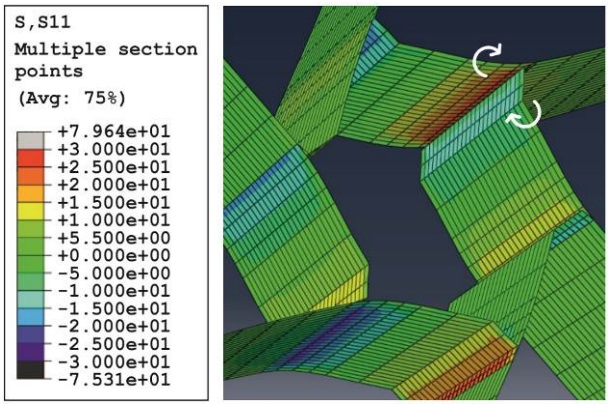

Fig. 3 – Contour of longitudinal stress in the walls of a chiral network with polygonal nodes in tensile conditions

A convergence study was also performed considering the same type of network presented in Fig. 3. The results, reported in Table 3, show that a difference of less than 1% exists between the model used to generate the data for Table 2 and a model with elements size reduced by a factor 2.

Table 3 – Convergence study for a model with hexagonal nodes

	Element size		
	0.75 mm	1.5 mm	3 mm
Stiffness (N/mm)	76.7	77.4	79.3

The results obtained with r = 5 and L = 25 mm were confirmed by considering three other hexa-chiral topologies, with the characteristics reported in Table 4. The same numerical approach was applied to the models representing the new chiral networks. An identical thickness of 0.2 mm was attributed to the ligaments, whereas the thickness of the hexagon walls was progressively increased. The results are reported in Fig. 4, where it can be seen that a Poisson's ratio close to -1 can be obtained with a wall thickness of 0.8 mm attributed to the nodal walls. The stiffness of the chiral network is also affected by such variable, although a maximum increment of 25% is observed when the thickness of the hexagon walls is increased from 0.4 mm to 0.8 mm.

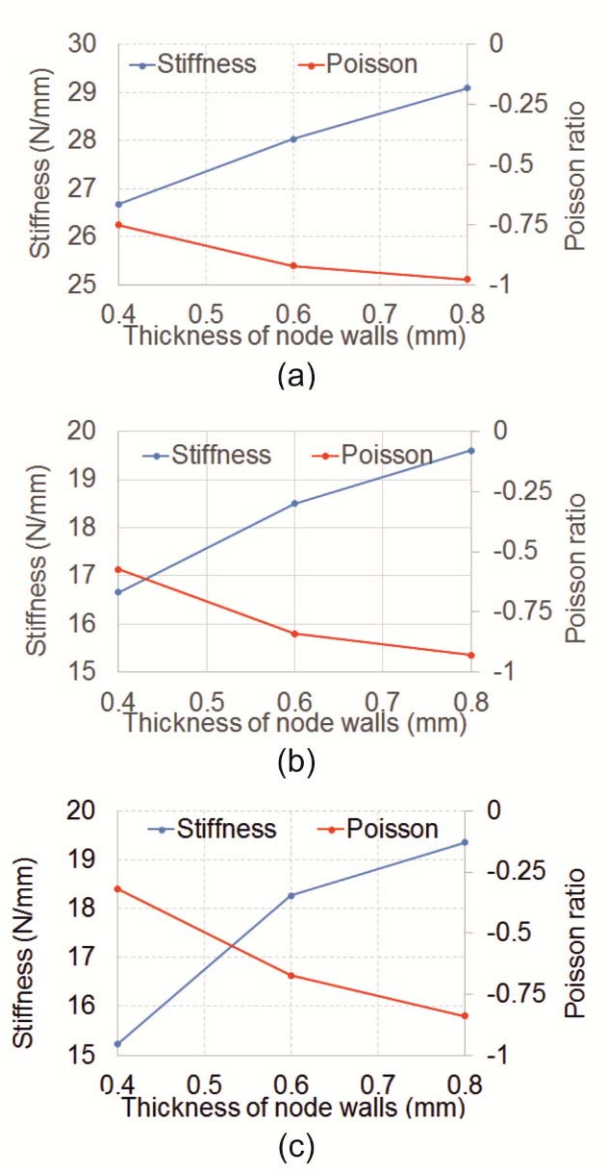

Fig. 4 – Stiffness and Poisson's ratio for three chiral topologies with hexagonal nodes as a function of the thickness of hexagon walls

Table 4 –Hexa-chiral configurations selected for numerical studies

Type	Hexagon apothem, *r*	Ligament length, *L*	*r/L*	Ligament length to thickness ratio

	(mm)	(mm)		
A	5	25.0	0.20	125
B	7	29.2	0.24	146
C	10	30.0	0.33	150

Actually, these preliminary studies do not take into account the real features of the networks that can be obtained by applying a technological process based on adjoining composite triangular tubes. In fact, such process will obtain ligaments with a thickness doubled with respect to the one of the nodal walls. This will lead to configurations with compliant nodes and stiff ligaments, with a detrimental effect on auxetic response.

A solution can be found by filling the interior of the nodes with a resin, after the production of the network. Such approach will stiffen the nodes and will also fill the cusps, which are the weakest point in the assembled element. Therefore, introduction of a filler in the nodes will lead, in the new technological approach, both to an improvement of auxetic performances and to an enhancement of mechanical strength.

Accordingly, a further numerical study was performed considering a topology with r and L selected according to the type A geometry reported in Table 4, a ligament thickness of 0.4 mm and a thickness of 0.2 mm in the hexagon walls. The ligaments were characterized by considering a $[0]_2$ lay-up of a carbon fabric pre-preg and a lay-up of $[0]_4$ for a glass fabric pre-preg. The properties of both materials are summarized in Table 1, although the cured ply thickness for the glass fabric pre-preg was adjusted to 0.50 mm to obtain the required thickness.

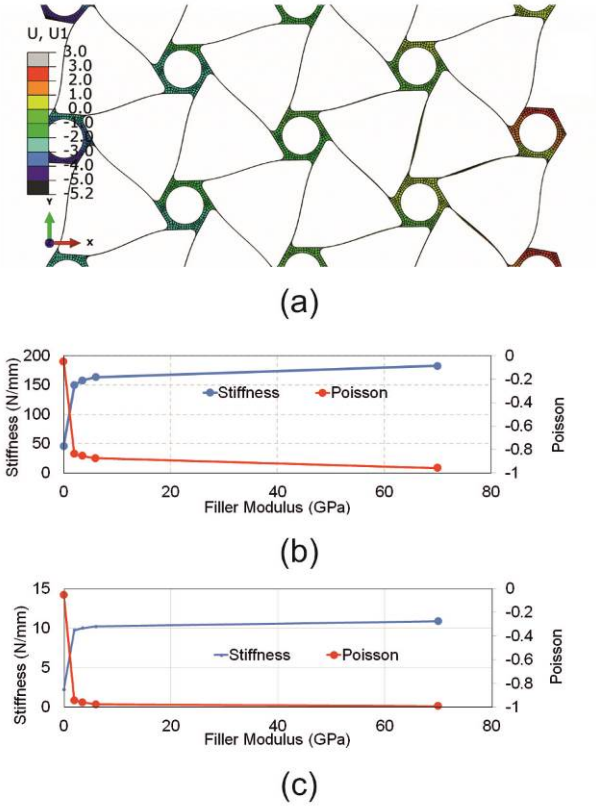

Fig. 5 – Finite element model of a chiral network with filled hexagonal nodes (a) and numerical mechanical properties for carbon (b) and glass (c) reinforced network with different fillers

Modelling techniques and application of boundary conditions were similar to the ones adopted for the previously considered network, but all the nodes were filled by a mesh of solid elements (*C3D8* elements [19]), with boundary nodes merged with the ones of the shells that represent the thin walls of the hexagons. A circular hole was considered at the centre of the filler, to reduce the additional weight cost due to the introduction of the filling material. The thickness of the filler in the nodes turns out to be in the range 1 mm ÷ 2 mm. A detail of the model is presented in Fig. 5-a, where the contour of the displacement in the horizontal direction is shown. A sensitivity study was performed for both carbon- and glass-reinforced chiral networks, by varying the Young modulus attributed to the filler material, which was considered isotropic with a Poisson's ration of 0.3. The results of this study are presented in Fig. 5-b

and 5-c for the networks modelled with carbon- and glass-reinforced ligaments, respectively. It can be concluded that the introduction of a filler with a Young Modulus of 3.5 MPa, which is a typical value for epoxy resins, leads to a Poisson's ratio close to -1. The results of the original configurations, without filler, are plotted in correspondence of a null Young Modulus. Such configurations were characterized by a significant nodal distortion and the Poisson's ratio of the network turned out to be close to zero. It can be seen that the addition of the filler, even with a low Young modulus, introduced a dramatic reduction of Poisson's ratios and an increment of the overall stiffness for both the networks considered in Fig. 5-b and Fig. 5-c.

4 Technological and experimental assessment of the new version of chiral composite honeycomb

The results obtained in the preliminary numerical studies motivated the development of a novel approach for the production of thin-walled composite chiral networks with reinforced polygonal nodes. A three-step technological process was devised, which consists of the separate production of composite triangular tubes, the subsequent assembly by bonding and the final application of reinforcement resin into the hexagonal nodes. Since the new configuration inherently reduces the risk of debonding between the assembled parts, a simple bonding process was applied, by using a cold curing adhesive. Although the adoption of the original high-temperature curing adhesive film, used in Bettini et al. [14], is still possible within the new process, such simplification facilitated the assembly phase and allowed a better control of the bonding procedure. A chiral topology with r = 5 mm, representing the hexagon apothem, and L = 25 mm was selected for the production of a chiral network consisting of 36 adjoined triangular tubes with a height of 20 mm.

The production of thin-walled composite tubes was carried out with the mandrel shown in Fig. 6-a. A first set of composite tubes was produced by using a carbon-reinforced fabric, SEAL CC90/ET443, with a $[0]_2$ lay-up, a nominal thickness of 0.20 mm and properties pro-

vided in Table 1. Additionally the E-glass-reinforced fabric SEAL EE48 REM, with the properties reported in Table 1, was used to produce another set of triangular tubes with a $[0]_4$ lay-up, corresponding to a nominal thickness of 0.22 mm. The tubes produced were subsequently cut to obtain the 20 mm height elements to be assembled in the second phase of the process. The rubber inserts for the application of pressure during the bonding process were easily produced by pouring the liquid silicon elastomer inside the tubes. The same silicon rubber used by Bettini et al. and by Airoldi et al. in previous chiral units manufacturing processes [14, 18] was adopted. Thereafter, a preliminary assembly was carried out to produce the external elastomeric frame that contains the assembled network.

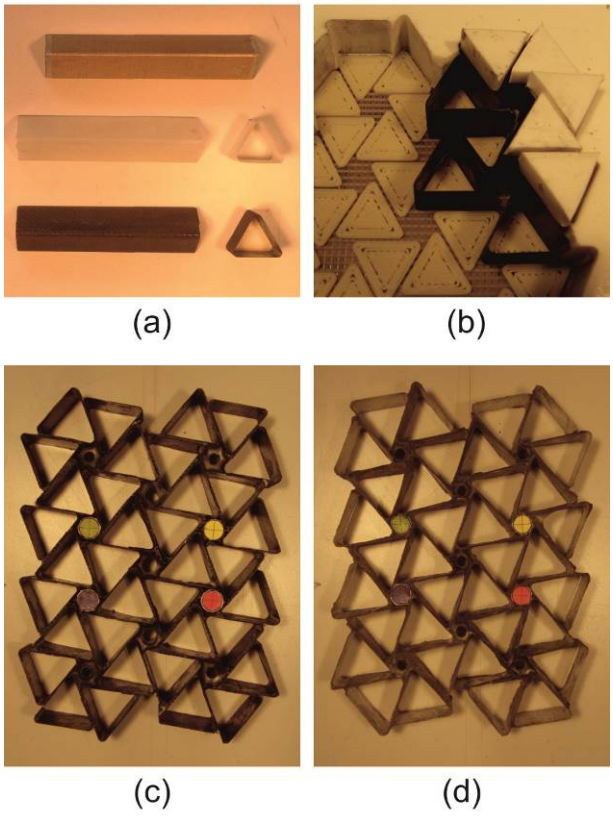

Fig. 6 – Production of thin-walled composite tubes (a), assembly of the chiral network (b) and produced units with carbon fabric (c) and glass fabric (d) ligaments

Assembly was carried out with the help of a positioning tool made of ABS polymer, produced by rapid prototyping, which is visible in Fig. 6-b.

Final assembly was performed after the application of an adhesive paste 3M/DP190 to the side of the triangular tubes. A vacuum bag was used to apply pressure during the curing of the adhesive, which was performed at room temperature. In the third phase of the process, the networks produced were extracted from the mould and the hexagonal nodes were filled by a cold curing epoxy system, made of Araldite® LY 5052 resin and Aradur® 5052 hardener. After curing, the nodes were drilled to remove the central part of the filler in each node. Figures 6-c and Fig. 6-d show two finished chiral networks with carbon- and glass-reinforced composite ligaments, respectively.

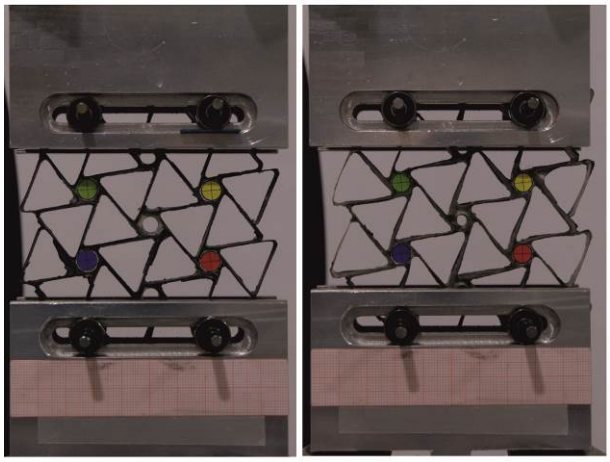

Fig. 7 – Test performed on a carbon-reinforced (a) and a glass-reinforced network (b)

The mechanical performance of the networks was evaluated by using the rig shown in Fig. 7. Four hexagonal nodes at the upper and lower end of the networks were pinned by means of 4 mm diameter steel rods. The ends of such rods were inserted into roller bearings that were able to translate along guides machined in two steel supports. The fixture was connected to an MTS 858 servo-hydraulic test system, which was used to perform tensile and compressive tests in displacement control mode, at a loading rate of 1,0 mm/min. The constraint system was devised to allow a free transverse expansion or contraction of the network. Poisson's ratio was measured considering the displacements of the four centres of the chiral nodes in the middle of the network, which were marked by coloured targets, as it shown in Fig. 7. Dis-

placements were evaluated by analysing the images taken by a fixed camera during the tests. A Matlab^{TM} tool for image analysis was used to evaluate the displacement from the coordinates of the pixels in the sequence of digital pictures. Such displacement were used to calculate the total engineering strains at the maximum loads, so to evaluate the experimental Poisson's ratios. It is worth noting that the networks and the load conditions in the experiments are different from the ones considered in the numerical studies presented in Section 3. In the numerical studies, the nodes at the boundaries of the network were considered complete and included in the models, and loads were applied to three upper nodes, whereas three lower nodes were constrained. Conversely, in the manufacturing process, nodes are created by the adjoined triangles and do not exist at the boundaries. For such a reason, loads and constrains were applied to two couples of internal nodes. The behaviour of the ligaments at the sides of the network is expected to be different with respect to the case considered in the numerical studies.

Figure 7-a is referred to a tensile test on a carbon-reinforced network, whereas Fig. 7-a was taken during the compressive test of a glass-reinforced network. The thickening that can be observed in some locations is the visual effect of a very thin membrane produced by the adhesive paste, which penetrated below the silicon rubber inserts under the pressure exerted by the vacuum bag. Such membrane has a thickness of the order of 1÷2 tenth of millimetres and the effects on the mechanical response were considered negligible.

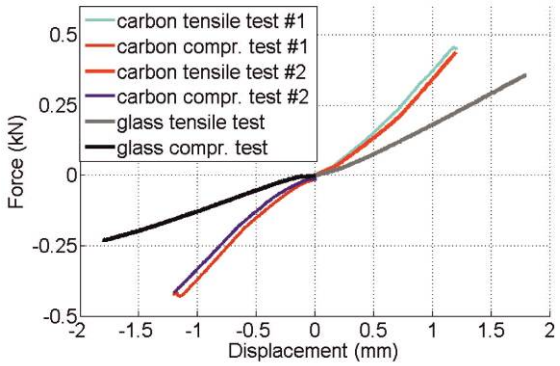

Fig. 8– Experimental force vs. displacement responses of the chiral networks

The forces vs. displacement curves obtained in the experimental tests are presented in Fig. 8. Curves indicate a symmetrical behaviour in tension and compression with non-linearities in the initial phase. Such behaviour can be attributed to geometrical imprecisions, which involve an initial adjustment to correctly distribute the loads between the left and right loading pins. After the initial adjustment, the response is linear. Tests were conducted until force levels with a magnitude of 0.5 kN and 0.3 kN for the carbon- and the glass-reinforced units, respectively, without detecting any type of failure in the central parts of the network. The weakest points in the components are represented by the cusps at the junctions between the external triangles, which are not protected by any reinforcement, since no hexagonal nodes exist at the lateral boundaries. For such a reason, the produced components cannot be considered adequate to evaluate the strength of the new technological concept.

5 Finite element analyses of the performed experiments

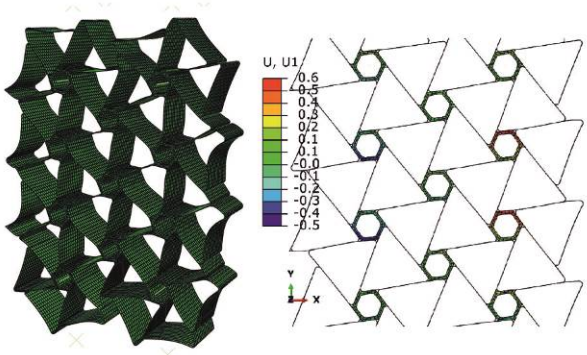

Fig. 9– Finite element model of the test (a) and numerical contour of transverse displacement (b)

Tests were also analysed by means of finite element models, as the one shown in Fig. 9-a. The contour reported in Fig. 9-b is referred to the transversal displacements in an analysis of a tensile test. In the models, an accurate representation of the network geometries was not attempted, considering the uncertainties related to the thickness of the resin in the nodal reinforce-

ment, to the properties of the adhesive layers set between the adjoined triangles and to the effect of ply overlaps in the very thin laminates that constitutes the triangular tubes. Nominal thickness was adopted for the composite plies, but an additional layer, with a Young modulus of 3.5 MPa and a Poisson's ratio of 0.3, was included at the middle of the ligament lamination sequence, to take into account the effect of the adhesive. The internal reinforcement of the hexagons was schematically represented by using two layers of solid elements, as it is shown in Fig. 9-b. The properties attributed to such layer, which is generally thinner than the real resin reinforcement, and the thickness of the adhesive layer interposed at the mid-plane of the ligaments were varied to improve the numerical-experimental correlations.

The boundary conditions applied to the network were based on the same constraint system that was used in the numerical studies, which was previously described. However, the pins were physically represented in these analyses, by using beams with axes passing through the centres of the four constrained nodes. A kinematic link that allows the rigid rotation of the constrained nodes was set between the central node of each pin and all the finite element nodes belonging to the constrained hexagons. Finally, the end nodes of the beams representing the pins were pinned to a set of reference nodes, where external constrains were applied. A vertical common displacement was attributed to the upper reference nodes, whereas the lower ones were kept fixed. Horizontal expansion and contraction of the networks were allowed, as in the experimental lay-out.

The experimental results of the tensile tests are reported in Table 5, in terms of stiffness and Poisson's ratios, together with the numerical results that were obtained by attributing a Young modulus of 10 GPa to the equivalent reinforcement layer and a thickness of 0.15 mm to the layer of adhesive between the sides of triangles. The results reported indicate that such approach leads to a general good correlation, with the exception of the Poisson's ratio for the carbon-reinforced network. The experimental setup allowed a measure of the transversal dis-

placements of the nodes and results are in reasonable agreement with the numerical predictions of the tuned model. Although Poisson's ratio are quite far from the -1 limit, the discrepancy with the Poisson's ratio predictions obtained in the previous section can be well explained considering that the networks used in the experimental test are significantly narrower than the ones used for numerical studies. Poisson's ratios are quite far from the -1 limit in both the numerical and the experimental results. The discrepancy with the Poisson's ratio predictions obtained in the previous section can be well explained considering that the networks used in the experimental tests, and in the related finite element models, are significantly different than the ones used for numerical studies, as it was previously remarked.

Table 5 – Stiffness and Poisson's ration of the chiral networks

	Carbon network Test #1	Carbon network Test #2	Glass network
Experimental stiffness (N/mm)	359	366	190
Experimental Poisson's ratio	-0.571	-0.572	-0.359
Numerical stiffness	367		184
Numerical Poisson's ratio	-0.403		-0.363

5 Concluding remarks

In this paper, previous results obtained in the design and manufacturing of simple chiral units and more complex components by using composite thin ligaments was critically analysed to develop of a new methodology for the production of thin-walled composite chiral networks. Such new approach disclosed the possibility of achieving different types of advantages by adopting a topology that can be obtained by adjoining polygonal shapes. The methodology, which can be applied to manufacture other types of chiral topologies, leads to tessellations

with polygonal nodes that can achieve the desired auxetic performances, providing that an adequate stiffness is attributed to the nodes.

Since the technological process based on the new approach tends to obtain thick ligaments and relatively thin nodes, the problems related to node distortion were pointed out and solved by considering the possibility of filling the polygons by resin. According to the numerical results, even a partial filling, with a limited weight cost, improves the auxetic behaviour with a Poisson's ratio that tends to the theoretical limit of -1. Moreover, the filler protects the cusps at the end of the junctions between the elements that constitute the network, so that the strength of the structure can be noticeably increased.

The technological activities confirmed the feasibility of the new approach. Although additional steps are required in the new process with respect to the original one, the precision of positioning is less critical and large networks can be more easily produced. A very promising feature is represented by the effect of the resin reinforcement applied to the interior of the nodes. Beneficial effects on the auxetic behaviour of such feature were numerically assessed and partially confirmed by experimental tests. Although the performed experiments were not adequate to provide a quantitative estimation of the real network strength, the analysis of the manufactured components and their behaviour during the tests provided indications that tensile strength levels could be higher than in the case of the superimposed ligaments produced with the original technology.

Overall, the studies carried out and the experimental activities presented in the paper indicate that the new process presents appealing characteristics regarding the simplification of the technological process, the achievement of Poisson's ratios close to the theoretical auxetic limit and the improvement of mechanical strength. Such promising results confirm that composite chiral networks have the potential to fulfil requirements regarding technological feasibil-

ity, functional performances and strength levels for future applications in the field of morphing aerospace structures.

References

[1] K. W. Wojciechowski, Constant thermodynamic tension Monte Carlo studies of elastic properties of a two-dimensional system of hard cyclic hexamers, *Molecular Physics*, **61**(5), 1247–1258 1987.

[2] K. W. Wojciechowski, C. Branka, Negative Poisson's ration in two dimensional "isotropic" solid, *Phyiscal Review A*, **40**(12), 7222-7225, 1989.

[3] R.S. Lakes, Deformation mechanism in negative Poisson's ratio materials : structural aspects, *Journal of Materials Science and Technology*, **26**, 2287-2292, 1991.

[4] D. Prall and R.S. Lakes, Properties of a chiral honeycomb with a Poisson's ratio -1, *International Journal of Mechanical Science*, **39**, 305-314, 1996.

[5] A. Alderson, K. Alderson, D.D. Attard, K. Evans, R. Gatt, J. Grima et al, Elastic constants of 3-,4- and 6-connected chiral and anti-chiral honeycombs subject to uniaxail in-plane loading, *Composite Science and Technology*, **70**(7), 1042-1048, 2010.

[6] A.A. Pozniak, K. W. Wojciechowski, Poisson's ratio of rectangular anti-chiral structures with size dispersion of circular nodes, *Physica Status Solid b*, **251**(2), 367-374, 2014.

[7] S. Barbarino, O. Bilgen, R.M. Ajaj, M.I. Friswell and D.J. Inman, A review of morphing aircraft, *Journal of Intelligent Material Systems and Structures*, **22**, 823-827, 2011.

[8] A.Y.N. Sofla, S, M.A. Meguid, K.T. Tan, W.K. Yeo, Shape morphing of aircraft wing: Status and challenges, *Materials and Design*, **31**, 1284-1292, 2010.

[9] D. Bornengo, F. Scarpa, C. Remillat, Evaluation of hexagonal chiral structure for moprhing airfoil concept, *Journal of Aerospace Engineering*, **219**, 185-192, 2005.

[10] J. Martin, J.J. Heyder-Bruckner, C. Remillat, F. Scarpa, K. Potter and M. Ruzzene, The hexachiral prismatic wingbox concept, *Physica Status Solidi B*, **245(**3**)**, 570-577, 2008.

[11] A. Spadoni and M. Ruzzene, Numerical and experimental analysis of chiral truss-core airfoils, *Journal of Mechanics of Materials and Structures*, **2**(5), 965-981, 2007.

[12] A. Airoldi, G. Quaranta, A. Beltramin and G. Sala, Design of a morphing actuated aileron with chiral composite internal structures, *Advances in Aircraft and Spacecraft Science*, **1** (3), 329-349,2014.

[13] A. Airoldi, M. Crespi, G. Quaranta, G. Sala. Design of a morphing airfoil with composite chiral structure, *Journal of Aircraft*, **49(**4**)**, 1008-1019, 2012.

[14] P. Bettini, A. Airoldi, G. Sala, L. Di Landro, M. Ruzzene and A . Spadoni, Composite Chiral Structures for Morphing Airfoils: Numerical Analyses and Development of a Manufacturing Process, *Composites Part B - Engineering*, **41**(2), 133-147,2010.

[15] W. Miller, C.W. Smith, F. Scarpa, K.E. Evans, Flatwise buckling optimization of hexachiral and tetrachiral honeycombs, *Composite Science and Technology*, **70**(7), 1049-1056, 2010.

[16] B. Caulfield, P.E. McHugh, S. Lohfeld, Dependence of mechanical properties of polymide components on build parameters in the SLS process, *Journal of Materials Processing Technology,* **182**, 477-488, 2010.

[17] G. Cicala , G. Recca, L. Oliveri, Y. Preikleous, F. Scarpa, C. Lira, A. Lorato, D.J. Grube and G. Ziegmann, Hexachiral truss-core with twisted hemp yarns : out-of-plane shear properties, *Composite Structures*, **94**, 3556-3562, 2012

[18] A. Airoldi, P. Bettini, M. Zazzarini, F. Scarpa, *Failure and Energy Absorption of Plastic and Composite Chiral Honeycombs*, in: Structures Under Shock and Impact XII, G. Schleyer and C.A. Brebbia (Eds.), WIT Press, Southampton, 2012.

[19] Abaqus, *Analysis and User's Manual Version 6.13*, 2013.

[20] E. Andreassen, B.S. Lazarov, O. Sigmund, Design of manufacturable 3D extremal elastic microstructure, *Mechanics of Materials,* **69**, 1-10, 2014.

[21] T. Strek, H. Jopek, B.T. Maruszewski, M. Nienartowicz, Computational analysis of sandwich-structured composites with an auxetic phase, *Phyisica Status Solidi B,* **251**(2), 354-366, 2014.

[22] T. Strek, H. Jopek, M. Nienartowicz, Dynamic response of sandwich panels with auxetic cores, *Phyisica Status Solidi B,* DOI 10.1002/pssb.201552024 (2015)